

UC Davis

UC Davis Previously Published Works

Title

The Use of Mouse Models of Breast Cancer and Quantitative Image Analysis to Evaluate Hormone Receptor Antigenicity after Microwave-assisted Formalin Fixation

Permalink

<https://escholarship.org/uc/item/9k99b636>

Journal

Journal of Histochemistry & Cytochemistry, 62(5)

ISSN

0022-1554

Authors

Engelberg, Jesse A
Giberson, Richard T
Young, Lawrence JT
et al.

Publication Date

2014-05-01

DOI

10.1369/0022155414529250

Peer reviewed

The Use of Mouse Models of Breast Cancer and Quantitative Image Analysis to Evaluate Hormone Receptor Antigenicity after Microwave-assisted Formalin Fixation

Jesse A. Engelberg, Richard T. Giberson, Lawrence J.T. Young, Neil E. Hubbard, and Robert D. Cardiff

Center for Comparative Medicine, University of California, Davis, California (JAE,LJTY,NEH,RDC); and Research and Development, Ted Pella, Inc., Redding, California (RTG)

Summary

Microwave methods of fixation can dramatically shorten fixation times while preserving tissue structure; however, it remains unclear if adequate tissue antigenicity is preserved. To assess and validate antigenicity, robust quantitative methods and animal disease models are needed. We used two mouse mammary models of human breast cancer to evaluate microwave-assisted and standard 24-hr formalin fixation. The mouse models expressed four antigens prognostic for breast cancer outcome: estrogen receptor, progesterone receptor, Ki67, and human epidermal growth factor receptor 2. Using pathologist evaluation and novel methods of quantitative image analysis, we measured and compared the quality of antigen preservation, percentage of positive cells, and line plots of cell intensity. Visual evaluations by pathologists established that the amounts and patterns of staining were similar in tissues fixed by the different methods. The results of the quantitative image analysis provided a fine-grained evaluation, demonstrating that tissue antigenicity is preserved in tissues fixed using microwave methods. Evaluation of the results demonstrated that a 1-hr, 150-W fixation is better than a 45-min, 150-W fixation followed by a 15-min, 650-W fixation. The results demonstrated that microwave-assisted formalin fixation can standardize fixation times to 1 hr and produce immunohistochemistry that is in every way commensurate with longer conventional fixation methods. (*J Histochem Cytochem* 62:319–334, 2014)

Keywords

model system, formalin, microwave, quantitative image analysis, breast cancer, mouse, antigenicity

Introduction

The methods and quality of tissue fixation can significantly affect tissue morphology and antigenicity, factors that are important in both research and clinical pathology. In addition to morphological factors such as tumor grade, pathologists assess the amount of hormone receptor proteins within invasive tumor cells to provide prognostic information. The overall quality of fixation can be assessed by many parameters, including morphology, antigenicity, and molecular data. When changing a single component of an established protocol, it would be ideal to quantify these parameters, instead of only relying on subjective assessment by

pathologists. A number of semi-quantitative measurements of antigenicity have been proposed and tested for breast cancer, including: Allred Score (Allred et al. 1998), J-Score (Kurosumi 2007), H-score (McClelland et al. 1990), and “quickscore” (Leake et al. 2000) methods. These are all based on the percentage of positive tumor cells and, except

Received for publication August 5, 2013; accepted February 24, 2014.

Corresponding Author:

Robert D. Cardiff, M.D., Ph.D., Center for Comparative Medicine, University of California Davis, One Primate Drive, Davis, CA 95616.
E-mail: rdcardiff@ucdavis.edu

for J-Score, all apply a “label intensity” component to the scoring.

Recently, we developed methods for quantitative image analysis (QIA) that provide a quantitative description of staining intensity over an entire tissue sample (Cardiff et al. 2013). Our Density:Intensity histograms were validated in a lengthy study on mouse and human breast cancers (Cardiff et al. 2013). In this study, we use the new QIA technology to measure antigenicity when mouse tissues were fixed with or without the application of microwave energy. Microwave-assisted (MA) formalin fixation with 10% neutral buffered formalin (NBF), containing approximately 4% formaldehyde, has been demonstrated to reduce fixation times to as little as 20 min without affecting morphology or vimentin antigenicity of paraffin-embedded tissues (Galvez et al. 2006). An MA approach to NBF fixation saves considerable time over conventional methods of NBF fixation (Fox et al. 1985) and provides the additional benefit of standardizing the fixation step to a single time point (Giberson and Elliott 2001; Galvez et al. 2006; Gagna et al. 2007). This is particularly relevant because the debate over minimum and maximum formalin fixation times, especially in breast cancer diagnostics, has been extensive and ongoing (von Wasielewski et al. 1998; Goldstein et al. 2003; Wolff et al. 2007; Gown 2008; Yaziji et al. 2008; Hammond et al. 2010; Tong et al. 2011; Nofech-Mozes et al. 2012).

To evaluate antigenicity, a four-antigen panel (IHC4) was employed, which is significant to the prognosis and treatment of breast cancer (Cuzick et al. 2011). The IHC4 panel consists of (1) estrogen receptor (ER), (2) progesterone receptor (PR), (3) human epidermal growth factor receptor 2 (Her2), and (4) the proliferation and ribosomal RNA transcription protein (Ki67). The acquisition of digital whole slide images (WSI) followed by proven methods of QIA (Cardiff et al. 2013) provided the means to evaluate the antigenicity of the IHC4 panel after the different fixation methods.

The findings of this study provide a quantitative and graphical basis of comparison for each fixation method and antigen consistent with the microscopic evaluation of the results. The use of QIA on WSI provided an unbiased reproducible means of quantifying antigenicity that clearly indicated that MA NBF fixation would produce IHC4 labeling results in 1 hr that are equivalent to those achieved with conventional 24-hr fixation.

Materials & Methods

This study employed two mouse models of breast cancer to evaluate antigenicity after fixation with 10% NBF by either MA or conventional room temperature techniques. We compared two 1-hr MA methods of NBF fixation (Giberson and Elliott 2001; Galvez et al. 2006; Gagna et al. 2007) to a

passive soaking in NBF at room temperature for 24 hr (the control). After fixation, the tissues were placed in 70% ethanol and processed into paraffin. Together, the two mouse models expressed all four IHC4 antigens. We utilized a rigorous, established standard operating procedure (SOP) for all steps, from tissue acquisition through processing and labeling, in addition to proven methods of QIA to quantify and characterize labeling intensity and density (Cardiff et al. 2013).

Mouse Models

The two mice used for these two models of human breast cancer were housed at the Center for Comparative Medicine Mouse Biology Program at the University of California, Davis. All procedures were performed in accordance with the U.S. Public Health Service Policy of Humane Care and Use of Laboratory Animals as well as the Animal Welfare Act (7 U.S.C. et seq.). Animal use protocols were approved by the Institutional Animal Care and Use Committee of the University of California, Davis.

Mouse Mammary Tumor Cell Lines

The two mouse mammary tumor cell lines used in this study were:

- 1) SSM2 (ER/PR positive, Ki67⁺, Her2^{Low}): Luminal-like tumor from Tm (Stat1^{-/-} (Schreiber/Chan)) (Taconic, Hudson, NY) (Chan et al. 2012).
- 2) NDL (Her2⁺, Ki67⁺, ER/PR negative): Luminal-like tumor line from Strain FVB mice with a *neu* deletion (NDL) allele Tg(MMTV:NDL^{Muller}) (Siegel et al. 1999).

The two tumor cell lines were grown in culture and prepared for transplantation into the #3 and/or #4 mouse mammary fat pads. The two tumor lines were transplanted into each wild type mouse and allowed to grow prior to processing and evaluation. For all experiments, mammary gland, uterus, and liver were sampled.

Animals were sacrificed with a lethal dose of intraperitoneal pentobarbital sodium. Tumor, mammary gland, uterus and liver were removed, each divided into 2-mm pieces, and placed in NBF as quickly as possible after sacrifice. In all cases, the time from sacrifice to immersion in NBF was less than 30 min. Three tissue pieces (tumor/mammary gland, uterus, and liver) from each animal were placed into each of 6 cassettes. These served as replicates for the three fixation protocols: (1) MA 60 min at 150 W, (2) MA 45 min at 150 W followed by 15 min at 650 W, and 24 hr control fixation at room temperature. To differentiate amongst the processing groups, the tumors from each mouse model tumor were designated ‘A’ and ‘B’.

Microwave-assisted NBF Fixation

Microwave-assisted NBF fixation was performed with a PELCO BioWave® Pro (Ted Pella, Inc., Redding, CA). The microwave processor can be programmed to deliver continuous power at any power output from 100 to 750 W. Power delivery is, therefore, continuous throughout the fixation process versus on/off or pulsed. Continuous sample temperature control during microwave exposure was obtained through the use of the PELCO SteadyTemp™ Pro (STP, Ted Pella, Inc., Redding, CA). This ancillary device functions as a chiller or heater and is connected to the microwave via fluid hoses for circulation and an RS 232 cable. The STP circulates and controls the temperature of a 2 L volume of water in an 8.25-inch square × 4-inch deep polypropylene container inside the microwave cavity.

Two different MA protocols, previously demonstrated to preserve tissue ultrastructure were evaluated: 1) 60 min at 150 W and fixative temperature <37C; MW1-A for Tumor A and MW1-B for Tumor B; 2) 45 min at 150 W + 15 min at 650 W and fixative temperature <37C; MW2-A for Tumor A and MW2-B for Tumor B (Giberson and Elliott 2001; Galvez et al. 2006).

Tissues for fixation were placed in 50 ml conical screw cap tubes (USA Scientific Inc., Ocala, FL) containing 45 ml of NBF. The tubes floated on their sides in the container cooled by the STP inside the microwave cavity. In this way, no agitation of the NBF took place during microwave exposure. To maintain NBF temperatures below 37C inside the screw cap tubes for the 150 W cycle, the STP was set at 26C. The 150/650 W cycle required that the STP automatically reset to 10 C for the 650 W portion of the cycle to maintain the final NBF temperature below 37C inside the tube.

Control NBF Fixation

Tissues fixed as controls were placed in cassettes and allowed to sit in NBF at room temperature (approximately 23C) for a 24-hr passive fixation. Controls for each mouse model were designated Control-A for one tumor and Control-B for the other. In this way they directly correspond with the MA processing groups. Passive relates to the fact that no agitation of the sample or fixative was performed during the period. Minimum conventional NBF fixation times for the IHC4 are from 6-8 hr (von Wasielewski et al. 1998; Werner et al. 2000; Goldstein et al. 2003; Wolff et al. 2007; Gown 2008; Yasiji et al. 2008; Nofech-Mozes et al. 2012).

Tissue Processing after Fixation

Immediately after fixation, the tissues were transferred to 70% ethanol before overnight processing into paraffin with

a Tissue-Tek autoprocesor (Sakura Finetek USA, Inc., Torrance, CA). Each cassette contained a sample of tumor/mammary gland, uterus, and liver.

The tissues were embedded in Paraplast paraffin (melting temperature 56–60C), sectioned to 5 µm and mounted on glass slides. Sections were stained using Mayer's hematoxylin and eosin (H&E) to facilitate evaluation of histology and morphology. During processing, tissues were dehydrated in a graded series of ethanol and cleared with xylene prior to paraffin infiltration.

All pre- and post-fixation steps were standardized by having them performed by a single individual.

Immunohistochemistry

All tissues were stained for IHC4 by a single individual. All primary antibodies were rabbit polyclonal and the source and dilutions are listed below.

- 1) ER: Santa Cruz Biotechnology, Inc., Dallas, TX (Cat# sc-542; dilution 1:800).
- 2) PR: Dako North America, Inc., Carpinteria, CA (Cat# A0098; dilution 1:500).
- 3) Ki67: Lab Vision (Neomarker), Fremont, CA (Cat# RB1510-PO; dilution 1:800).
- 4) c-erbB2 (Her2): Lab Vision (Neomarker), Fremont, CA (Cat# RB103-PIABX; dilution 1:600).

Slides for immunohistochemistry were deparaffinized in three changes of xylene followed by three changes of 100% EtOH followed by quenching for endogenous peroxidase with 3% hydrogen peroxide (20 ml of 30% H₂O₂ plus 180 ml of 100% methanol). Slides were then rehydrated with two stages each of 100%, 95% and 70% ethanol (2 min each step) followed by 5 min in running tap water and two rinses with distilled water. Antigen retrieval was performed with freshly-made citrate buffer, pH 6.0, in a Decloaking Chamber™ (Biocare Medical, Concord, CA). Slides were rinsed and then blocked with 10% horse or goat serum in phosphate-buffered saline (PBS) for 20 min. All primary antibodies were diluted with PBS + 0.1% Ova Albumin (Sigma-Aldrich, St. Louis, MO), and stained overnight at room temperature. Slides were rinsed in PBS and secondary antibody staining in PBS + 0.1% Ova Albumin was done for 1 hr at room temperature with biotinylated goat anti-rabbit IgG (Vector Laboratories, Burlingame, CA) at 1:1000 dilution.

After rinsing in PBS, slides were stained for 30 min at room temperature with avidin-biotin complex (ABC Reagent, Vector Laboratories, Burlingame, CA) in PBS + 0.1% Ova Albumin, rinsed in PBS, and treated with diaminobenzidine (Vector Laboratories, Burlingame, CA) for 3-5 min. Slides were then rinsed in water, counterstained with hematoxylin, dehydrated in ethanol, and cleared in xylene

before cover-slipping. Negative and positive controls were included with each run.

Control Tissues: ER, PR, Ki67 and ErbB2 (Her2)

Mouse uterine tissue was used for the positive and negative (primary antibody-deletion) immunohistochemistry controls for ER and PR. The uterine myometrium from the recipient mice was used as control tissue for ER/PR in each experiment because it is essentially constant through the estrous cycle (Cardiff et al. 2013). For each experiment, normal human tonsils and normal mouse lymph nodes served as positive and negative (primary antibody-deletion) controls for Ki67. The NDL mammary tumor overexpresses ErbB2 (Her2), and was chosen as the positive control. A standard NDL tumor block was used for each IHC run using anti-ErbB2 (Her2).

Whole Slide Images and Quantitative Image Analysis

After fixation and staining, slides were scanned to create digital whole slide images (WSI) using an Aperio ScanScope XT (Aperio Technologies, Vista, CA). The data from each slide was automatically captured and stored in the Aperio Spectrum version 11 database. Each WSI was annotated by experienced morphologists to select similar tumor, mammary gland and uterine tissue regions. All tissue regions in each WSI were analyzed using Aperio ImageScope software (<http://www.aperio.com/#imagescope-request>). The Aperio “Membrane” (ErbB2/Her2) and “Nuclear” (ER, PR and Ki67) version 9 algorithms were used to count the number of cells in total and measure the intensity of positive staining in each cell. The percentage of positively stained cells (and the 1+, 2+, and 3+ intensity breakdowns) in each tumor and uterus was calculated and recorded in the Aperio Spectrum database.

Aperio Algorithm Parameter Settings

The nuclear and membrane algorithms have parameters that can be changed to affect cell detection or to change the intensity cutoff values used to bin cells in the 1+, 2+, or 3+ categories. For tumor tissue we retained the default parameter settings to ensure consistency with our previous work in SSM2 and NDL mouse tissues (Cardiff et al. 2013) and also because they produced empirically valid results for cell detection and segmentation. The algorithm parameter settings were modified for the uterine myometrium to take into account the fusiform shape of the smooth muscle cells of the myometrium, which improved the accuracy of ER, PR, and Ki67 analyses (Cardiff et al. 2013). We used identical intensity cutoff values for all tissues, retaining the default intensity cutoff values to ensure consistency with previous

work, but also because the goal of the project was to assess variance in staining. As long as each sample was analyzed using the same cutoff values, similarly stained tissue should present similar histograms and percentage values.

Density: Intensity Line Plots

Intensity and cell count data were exported from Spectrum to create Density:Intensity line plots. These line plots were used in combination with percent positive data to evaluate the immunohistochemistry results in this study. The line plots represented the relative cell density (y-axis) at any given intensity (x-axis) for cells annotated for a given tissue. Because the line plots represent 256 intensity bins instead of 4 (0, 1+, 2+, 3+), they provide a more detailed interpretation of the staining distribution than percent positive data alone. The data were analyzed using R, a “freely available language and environment for statistical computing and graphics” (<http://www.R-project.org>). The plot produces a measure of “cell density” in cells/mm² versus intensity, measured from 0 (lightest) to 1 (darkest) in optical intensity units (OIU). For the nuclear algorithm, the cells with intensity above the cutoff value of 0.125 OIU were regarded as “positive staining” and less than 0.125 as “negative staining”, whereas, for the membrane algorithm, the cutoff value was 0.167 OIU. The line plots were smoothed using a loess predictor, which smoothed the data using locally weighted linear regression, with a span of 0.1 chosen empirically.

Kolmogorov-Smirnov Test to Assess Line Plot Similarity

The Kolmogorov-Smirnov (KS) test is a non-parametric test that can measure if two sample distributions were drawn from the same distribution or not (Kolmogorov 1933). The empirical distribution functions for both distributions are calculated and the distance between them compared. If that distance is greater than a critical level in the KS table, the null hypothesis that the distributions differ is rejected. The R *ks.test* library was used to calculate the *p* value for a two-sample KS test. Because we wanted to assess whether or not the microwave protocols would reduce antigenicity, we used the alternative hypothesis that the microwave sample was less than the control sample. Simply put, a small *p* value (less than 0.05) for the KS test would indicate that the microwave sample had lower antigenicity than the control sample. In addition to comparing the microwave and control tissues, the KS test was used to assess the biological variance between the two control fixations for the different tissues. In this case, the regular two-sample KS test was used, and small *p* values would indicate that the control samples differed. This approach provided insight into the variance in staining between any two tissues from the same mouse fixed using control methods.

Determination of Similarity by Microscopic Examination

The following considerations were used by experienced pathologists to determine similarity between the two fixation techniques:

- 1) Is the stain localization and counterstain appropriate and specific for each antigen?
- 2) Is there an equivalent staining intensity noted for both techniques for control and MA-fixed slides for all four antigens?
- 3) Is the background staining increased or decreased by MA fixation?
- 4) Would the results from MA fixation have changed the diagnosis or prognosis?

Results

This research employed well-characterized mouse models of breast cancer (Cardiff et al. 2013) and an IHC4 panel of antibodies that has been extensively studied and comes with rigorous assay requirements (Leake et al. 2000). Antigen preservation, as measured by labeling intensity, the line plots, cell density numbers and the Kolmogorov-Smirnov test of the line plots were the key determinants in this comparison of two fixation methods. The microscopic examination of the IHC4 stained slides was used to affirm the QIA results.

Quantitative Image Analysis of IHC4

The results of the IHC4 of mammary gland are not shown due to the small number of available nuclei (<1000) in 20 of the 36 tissue samples. All tumor or uterine samples evaluated had >1000 nuclei. The average number of nuclei evaluated was 20,147 for each tumor sample and 8,530 for the uterus.

Percent Positive Labeling

The Aperio “Membrane” (ErbB2/Her2) and “Nuclear” (ER, PR and Ki-67) version 9 algorithms were used for QIA. Labeling intensities (1+, 2+, 3+, and total percent positive) were calculated by QIA for each tissue and fixation method for IHC4. Currently, semi-quantitative methods serve as the basis for the IHC4 diagnostic and prognostic interpretation (Nofech-Mozes et al. 2012), including Allred Immunohistochemistry Score (Allred et al. 1998), J-Score (Kurosumi 2007), H-score (McClelland et al. 1990), and “quickscore” (Leake et al. 2000) methods. By calculating both the percent positive and the Density:Intensity line plots, we could compare antigenicity at the resolution used for diagnostic interpretation and also

at a much finer-grained resolution. The intensity levels used were the default cutoffs provided by the Aperio algorithm. The different labeling intensities (1+, 2+, 3+) and total percent positive cells were compiled and are presented in Table 1.

NDL Mouse Model Percent Positive Label

The NDL model overexpresses ErbB2 (Her2) to a degree that is relevant in the prognosis of human cancers. However, diagnostically, the ER/PR tumor staining would be considered negative, although there is some push to consider 1% positive staining for ER as positive (Nofech-Mozes et al. 2012). All 6 samples of tumor presented ER staining from 1 to 2.8% positive. Tumor PR labeling was from 0 to 1.9% for all samples (Control-A, 0%; Control-B, 0.2%). The ErbB2/Her2 tumor staining results were consistent across all samples for uniform intense and complete (59.6-72.8%) membranous staining (Gown 2008). Tumor percent positive results for Ki67 presented a range of values from a low of 40.8% for Control-B to a high of 59.4% for MW2-A. Uterine percent positive differences for all samples were within 4% for ER (except MW2-B), 7.4% for PR, and 2.1% for Ki67.

SSM2 Mouse Model Percent Positive Label

The SSM2 model is similar to human luminal cancer. The ER/PR tumor total percent positive staining differences for all samples were all within 6.9% for ER and 12.6% for PR. The range for 3+ label intensity for PR was >20% (low 30.9% for MW1-A, high 53.4% for MW1-B). The 3+ labeling intensity for PR, due to intra-tumor heterogeneity, can vary by over 20% (Cardiff et al. 2013). The MW2-A samples for ER and PR presented insufficient tissue (<1000 nuclei each) with which to provide valid intensity data. The Ki67 tumor values presented a range from a low of 28.3% for Control-B to a high of 40.5% for Control-A.

Uterus Control

The uterine labeling results for ER presented an approximate 10% difference between Control-A and B and MW2-A and B. The MW1-A to B difference was >10%. The uterine PR values presented a 43.1% spread (MW2-B lowest, MW1-B highest). The differences for MW1-A, MW2-A, and Control-A were all within 3%.

Density:Intensity Line Plots and Cell Density for the IHC4

The graphical representation of the staining data available via the Density:Intensity histograms provided more detailed information of the stain distribution. These plots (Figs. 1, 2)

Table 1. Percent Positive Labeling Data from the four-antigen panel (IHC4) of the ND1 and SSM2 Mouse Models.

		SSM2 Mouse Model																	
		Tumor A				Tumor B				Tumor A				Tumor B					
		MW1-A	MW2-A	Control-A	MW1-B	MW2-B	Control-B	MW1-A	MW2-A	Control-A	MW1-B	MW2-B	Control-B	MW1-A	MW2-A	Control-A	MW1-B	MW2-B	Control-B
ER																			
Intensity																			
1+		1.2	2.2	1.0	1.9	2.2	2.8	30.8		27.3	25.0	28.3	30.2						
2+		0.0	0.0	0.0	0.0	0.0	0.0	8.0	<1000	6.4	6.7	8.9	6.4						
3+		0.0	0.0	0.0	0.0	0.0	0.0	0.5	Nuclei	0.4	0.7	0.4	0.2						
Total		1.2	2.2	1.0	1.9	2.2	2.8	39.3		34.1	32.4	37.6	36.8						
PR																			
Intensity																			
1+		0.4	1.7	0.0	0.4	0.6	0.2	14.5		10.8	8.0	9.9	12.3						
2+		0.0	0.2	0.0	0.0	0.0	0.0	20.5	<1000	19.8	15.6	15.2	26.1						
3+		0.0	0.0	0.0	0.0	0.0	0.0	30.9	Nuclei	44.3	53.4	44.0	40.1						
Total		0.4	1.9	0.0	0.4	0.6	0.2	65.9		74.9	77.0	69.1	78.5						
Ki-67																			
Intensity																			
1+		14.5	14.0	12.7	16.3	15.6	14.7	12.1	13.1	12.4	12.9	12.6	13.4						
2+		14.7	18.0	15.0	18.1	17.7	14.8	12.7	11.8	13.6	13.2	13.2	10.0						
3+		13.8	27.4	23.9	15.5	23.7	11.3	12.5	10.4	14.5	11.3	11.1	4.9						
Total		43.0	59.4	51.6	49.9	57.0	40.8	37.3	35.3	40.5	37.4	36.9	28.3						
Her2																			
Intensity																			
1+		32.8	27.0	33.8	43.1	33.9	54.4												
2+		54.1	56.2	63.4	42.5	62.8	31.4												
3+		13.0	16.6	2.7	4.1	3.0	6.9												
Total		99.9	99.8	99.9	89.7	99.7	92.7												
% Complete		67.0	72.8	66.4	69.7	68.4	59.6												
ER																			
Intensity																			
1+		17.6	18.0	17.3	19.1	15.9	16.7	18.1	15.4	17.1	16.5	19.6	16.0						
2+		24.6	24.6	22.5	20.2	21.0	23.2	19.9	16.1	21.2	24.6	23.6	20.6						
3+		28.9	29.8	30.7	34.6	22.1	34.6	20.1	19.5	21.4	31.0	18.4	32.4						
Total		71.1	72.4	70.5	73.9	59.0	74.5	58.1	51.0	59.7	72.1	61.6	69.0						
PR																			
Intensity																			
1+		18.9	25.2	23.0	18.7	18.3	18.3	25.3	21.3	28.1	32.5	17.2	29.6						
2+		22.4	25.8	22.9	22.1	23.4	21.2	7.8	8.2	4.9	24.4	1.1	18.8						
3+		16.4	14.1	14.5	22.5	21.7	23.1	1.1	2.5	0.3	4.5	0	3.4						
Total		57.7	65.1	60.4	63.3	63.4	62.6	34.2	32.0	33.3	61.4	18.3	51.8						
Ki-67																			
Intensity																			
1+		0.5	1.5	0.9	2.4	1.3	1.9	1.9	5.6	4.0	3.5	3.6	3.4						
2+		0.3	0.4	0.5	0.5	0.2	0.3	1.4	2.6	1.8	2.3	1.4	1.9						
3+		0.4	0.5	0.4	0.4	0.3	0.3	1.2	1.3	1.1	1.8	0.8	0.8						
Total		1.2	2.4	1.8	3.3	1.8	2.5	4.5	9.5	6.9	7.6	5.8	6.1						

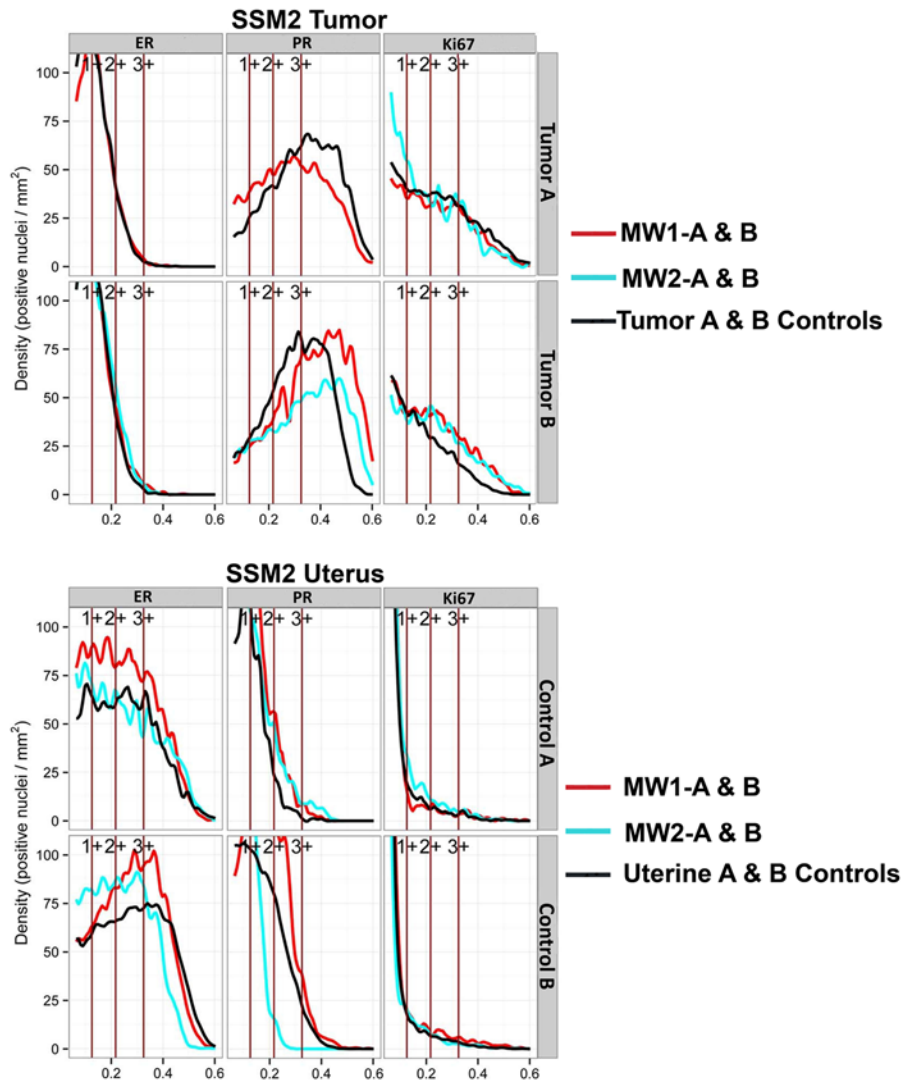


Figure 2. Density:Intensity line plots of the four-antigen panel (IHC4) from the SSM2 tumors and uterus. The SSM2 model is human epidermal growth factor receptor (Her2) negative. These plots represent the relative cell density in cells/mm² (y-axis) at any given intensity (x-axis) for the IHC4 of the SSM2 tumor and uterus. The intensity levels were the default cutoffs provided by the Aperio algorithm and the vertical lines represent 1+ >0.125 OIU, 2+ >0.217 OIU, and 3+ >0.325 OIU.

Kolmogorov-Smirnov Test

The p values for each comparison are presented in Table 3 (NDL and SSM2 tumors) and Table 4 (uterus). In both tables, the p values are presented in conjunction with the total percent positive and cell density values. P values less than 0.05 for microwave-to-control comparisons indicated that the MA fixation reduced antigenicity (KS test alternative hypothesis). For control-to-control comparisons, the first number in the p value column represents the alternative hypothesis (Control-B is the experimental and Control-A the reference) and the second number, the regular two-sample KS test. In both instances, $p < 0.05$ results would be indicative of biological variation in the control fixation results (Tables 3 and 4).

NDL Mouse Model

For the NDL tumors, all KS comparisons were similar, except for the Her2 MW2-B to Control-B and Control-B to Control-A values (Table 3). The Her2 Control-B to Control-A p values were $p < 0.05$ for both the alternate hypothesis and the regular two-sample KS test. The Ki67 tumor controls exhibited a higher degree of biological variance, based on p value, than any of the microwave results for that marker. The tumor ER and PR p values of the MA fixations and the control-to-control values were the best data set for similarity within the study.

The uterine results for ER/PR indicated good similarity across all MW1 or 2 comparisons with the controls (Table 4). The control-to-control p values for both markers

Table 2. Cell Density Values from the Line Plots for the NDL and SSM2 Mouse Models from Figures 1–2.

NDL Mouse Model		SSM2 Mouse Model																							
		Tumor A					Tumor B					Tumor A					Tumor B								
		MW1-A	MW2-A	Control-A	MW1-B	MW2-B	Control-B	MW1-A	MW2-A	Control-A	MW1-B	MW2-B	Control-B	MW1-A	MW2-A	Control-A	MW1-B	MW2-B	Control-B	MW1-A	MW2-A	Control-A	MW1-B	MW2-B	Control-B
ER	Intensity	92	167	82	130	169	218.0	1818	<1000	1817	687	1980	1924	1576	1490	1377	1626	1321	1414	1311	1608	1846	1408	1506	5198
	1+	0	5.9	0.8	5.7	3.5	3.3	474	<1000	427	504	408	2197	2037	1784	1718	1747	1747	1972	1625	2385	2221	1823	1506	5198
	2+	0	0.6	0	0.5	0	0	27	Nuclei	25	55	14	2583	2473	2432	2952	1839	4907	2937	1636	3007	1730	2866	1506	5198
	3+	92.0	173.5	82.8	136.2	172.5	221.3	2319	Nuclei	2269	2430	2346	6356	6000	5593	6296	5300	6323	6323	4572	7000	5797	6097	1506	5198
	Total	26	104	3.2	22	36	18.0	PR	<1000	752	667	873	5287	5198	4629	5571	5300	4730	4730	1411	2899	1552	2040	1506	5198
	PR	0	16	0.4	2.8	1	0.6	980	<1000	1374	1032	1854	1731	2014	1761	1646	1531	1383	1383	1411	2899	1552	2040	1506	5198
	1+	0	3.6	0	0.8	0	0	1386	<1000	3080	2984	2840	2050	2058	1758	1949	1955	1600	1600	246	2176	95	1294	1506	5198
	2+	26	123.6	3.6	25.1	37	18.6	4463	Nuclei	5206	4683	5567	5287	5198	4629	5571	5300	4730	4730	13	405	0	233	1506	5198
	Total	1156	901	853	1064	1082	1001	Ki-67	921	845	884	820	5287	5198	4629	5571	5300	4730	4730	1670	6595	1647	3567	1506	5198
	Ki-67	1169	1156	1009	1182	1226	1010	771	921	929	924	820	1169	1156	1009	1182	1226	1010	1010	845	946	884	820	1169	1156
	1+	1100	1761	1606	1016	1642	773	799	827	988	777	614	1100	1761	1606	1016	1642	773	773	988	825	777	300	1100	1761
	2+	3425	3818	3468	3262	3950	2784	2381	2474	2762	2585	1734	3425	3818	3468	3262	3950	2784	2784	2762	2738	2585	1734	3425	3818
	Total	3	7	167	3086	794	4303	Her2	921	845	884	820	3	7	167	3086	794	4303	4303	845	946	884	820	3	7
	Her2	9026	8850	10466	6798	7897	5009	794	921	929	924	820	9026	8850	10466	6798	7897	5009	5009	845	946	884	820	9026	8850
	1+	1419	1918	301	502	280	842	794	921	929	924	820	1419	1918	301	502	280	842	842	845	946	884	820	1419	1918
	2+	10446	10795	10931	10386	8966	10144	794	921	929	924	820	10446	10795	10931	10386	8966	10144	10144	845	946	884	820	10446	10795
	Total	SSM2 Mouse Model Uterus																							
	ER	ER					ER					ER					ER								
	Intensity	MW1-A	MW2-A	Control-A	MW1-B	MW2-B	Control-B	MW1-A	MW2-A	Control-A	MW1-B	MW2-B	Control-B	MW1-A	MW2-A	Control-A	MW1-B	MW2-B	Control-B	MW1-A	MW2-A	Control-A	MW1-B	MW2-B	Control-B
	1+	1576	1490	1377	1626	1321	1414	1917	1411	1311	1608	1846	1408	1576	1490	1377	1626	1321	1414	1311	1608	1846	1408	1576	1490
	2+	2197	2037	1784	1718	1747	1972	2108	1473	1625	2385	2221	1823	2197	2037	1784	1718	1747	1972	1625	2385	2221	1823	2197	2037
	3+	2583	2473	2432	2952	1839	2937	2128	1791	1636	3007	1730	2866	2583	2473	2432	2952	1839	2937	1636	3007	1730	2866	2583	2473
	Total	6356	6000	5593	6296	4907	6323	6153	4675	4572	7000	5797	6097	6356	6000	5593	6296	4907	6323	4572	7000	5797	6097	6356	6000
	PR	PR					PR					PR					PR								
	1+	1731	2014	1761	1646	1531	1383	2142	1649	1411	2899	1552	2040	1731	2014	1761	1646	1531	1383	1411	2899	1552	2040	1731	2014
	2+	2050	2058	1758	1949	1955	1600	664	632	246	2176	95	1294	2050	2058	1758	1949	1955	1600	246	2176	95	1294	2050	2058
	3+	1506	1126	1110	1976	1814	1747	93	193	13	405	0	233	1506	1126	1110	1976	1814	1747	13	405	0	233	1506	1126
	Total	5287	5198	4629	5571	5300	4730	2899	2474	1670	6595	1647	3567	5287	5198	4629	5571	5300	4730	1670	6595	1647	3567	5287	5198
	Ki-67	Ki-67					Ki-67					Ki-67					Ki-67								
	1+	40	108	54	162	102	124	174	424	258	291	279	236	40	108	54	162	102	124	258	291	279	236	40	108
	2+	21	29	28	31	19	19	123	202	119	191	112	132	21	29	28	31	19	19	119	191	112	132	21	29
	3+	23	35	27	28	21	20	105	97	74	153	62	59	23	35	27	28	21	20	74	153	62	59	23	35
	Total	84	172	109	221	142	163	402	723	451	635	453	427	84	172	109	221	142	163	451	635	453	427	84	172

Table 3. KS Statistic *P* Values Compared to Percent Positive and Cell Density Values for NDL and SSM2 four-antigen panel (IHC4) Results.

Sample 1	vs.	Sample 2	Tissue	Genotype	Stain	<i>p</i> value	Percent Positive ^{**}	Cell Density ^{***}
MW1-A	vs.	Control-A	Tumor	NDL	ER	0.83	1.2/1.0	92.0/82.8
MW2-A	vs.	Control-A	Tumor	NDL	ER	0.78	2.2/1.0	173.5/82.8
MW1-B	vs.	Control-B	Tumor	NDL	ER	0.83	1.9/2.8	136.2/221.3
MW2-B	vs.	Control-B	Tumor	NDL	ER	0.94	2.2/2.8	172.5/221.3
Control-B*	vs.	Control-A	Tumor	NDL	ER	0.73/ 0.99	2.8/1.0	221.3/82.8
MW1-A	vs.	Control-A	Tumor	NDL	PR	0.97	0.4/0.0	26.0/3.6
MW2-A	vs.	Control-A	Tumor	NDL	PR	0.91	1.9/0.0	123.6/3.6
MW1-B	vs.	Control-B	Tumor	NDL	PR	0.83	0.4/0.2	25.1/18.6
MW2-B	vs.	Control-B	Tumor	NDL	PR	0.91	0.6/0.2	37/18.6
Control-B*	vs.	Control-A	Tumor	NDL	PR	1.0/0.94	0.2/0.0	18.6/3.6
MW1-A	vs.	Control-A	Tumor	NDL	Ki67	0.32	43.0/51.6	3425/3468
MW2-A	vs.	Control-A	Tumor	NDL	Ki67	0.47	59.4/51.6	3818/3468
MW1-B	vs.	Control-B	Tumor	NDL	Ki67	0.28	49.9/40.8	3262/2784
MW2-B	vs.	Control-B	Tumor	NDL	Ki67	0.21	57.0/40.8	3950/2784
Control-B*	vs.	Control-A	Tumor	NDL	Ki67	0.071/0.14	40.8/51.6	2784/3468
MW1-A	vs.	Control-A	Tumor	NDL	Her2	0.62	99.9/99.9	10446/10931
MW2-A	vs.	Control-A	Tumor	NDL	Her2	0.83	99.8/99.9	10795/10931
MW1-B	vs.	Control-B	Tumor	NDL	Her2	0.07	89.7/92.7	10386/10144
MW2-B	vs.	Control-B	Tumor	NDL	Her2	<i>p</i> <0.05	99.7/92.7	8966/10144
Control-B*	vs.	Control-A	Tumor	NDL	Her2	<i>p</i> <0.05/ <i>p</i> <0.05	92.7/99.9	10931/10144
MW1-A	vs.	Control-A	Tumor	SSM2	ER	0.57	39.3/34.1	2319/2269
MW2-A	vs.	Control-A	Tumor	SSM2	ER	Nuclei<1,000		
MW1-B	vs.	Control-B	Tumor	SSM2	ER	0.99	32.4/36.8	2430/2346
MW2-B	vs.	Control-B	Tumor	SSM2	ER	0.78	37.6/36.8	2633/2346
Control-B*	vs.	Control-A	Tumor	SSM2	ER	0.78/0.99	36.8/34.1	2346/2269
MW1-A	vs.	Control-A	Tumor	SSM2	PR	<i>p</i> <0.05	65.9/74.9	4463/5206
MW2-A	vs.	Control-A	Tumor	SSM2	PR	Nuclei<1,000		
MW1-B	vs.	Control-B	Tumor	SSM2	PR	0.94	77.0/78.5	5480/5567
MW2-B	vs.	Control-B	Tumor	SSM2	PR	<i>p</i> <0.05	69.1/78.5	4683/5567
Control-B*	vs.	Control-A	Tumor	SSM2	PR	0.32/ <i>p</i> <0.05	78.5/74.9	5567/5206
MW1-A	vs.	Control-A	Tumor	SSM2	Ki67	0.09	37.3/40.5	2381/2762
MW2-A	vs.	Control-A	Tumor	SSM2	Ki67	0.10	35.3/40.5	2474/2762
MW1-B	vs.	Control-B	Tumor	SSM2	Ki67	0.94	37.4/28.3	2738/1734
MW2-B	vs.	Control-B	Tumor	SSM2	Ki67	0.73	36.9/28.3	2585/1734
Control-B*	vs.	Control-A	Tumor	SSM2	Ki67	<i>p</i> <0.05/ <i>p</i> <0.05	28.3/40.5	1734/2762

*Control to Control: 1st number, "one-sided" KS-test; 2nd number, "two-sided" KS-test.

**Total percent positive values from Table 1.

***Total cell density values from Table 2.

were less than the MA samples and *p*<0.05 for PR. These results were not apparent in the percent positive or cell density numbers (Tables 1–2). The MW1-A and MW2-A *p* values for Ki67 were *p*<0.05 but the MW1-B and MW2-B *p* values were high and the control-to-control values high. The lack of similarity for the MW1-A and MW2-A to Control-A data was not expected based on the line plots (Fig. 1), percent positive data (Table 1) or the cell density values (Table 2).

SSM2 Mouse Model

The ER results for the SSM2 tumors, even with the relatively low cell numbers for the MW2-A sample, clearly indicated a good correlation between microwave results and the controls. The PR results for this tumor demonstrated a high degree of biological heterogeneity between the controls, which can also be observed in the microwave results (Table 3) and is consistent with previous results

Table 4. KS Statistic *P* Values Compared to Percent Positive and Cell Density Values for NDL and SSM2 Uterine four-antigen panel (IHC4) Results.

Sample 1	vs.	Sample 2	Tissue	Genotype	Stain	<i>p</i> value	Percent Positive**	Cell Density***
MW1-A	vs.	Control-A	Uterus	NDL	ER	0.57	71.1/70.5	6356/5593
MW2-A	vs.	Control-A	Uterus	NDL	ER	0.57	72.4/70.5	6000/5593
MW1-B	vs.	Control-B	Uterus	NDL	ER	0.15	73.9/74.5	6296/6323
MW2-B	vs.	Control-B	Uterus	NDL	ER	0.24	59.0/74.5	4907/6323
Control-B*	vs.	Control-A	Uterus	NDL	ER	0.62/0.06	74.5/70.5	6323/5593
MW1-A	vs.	Control-A	Uterus	NDL	PR	0.94	57.7/60.4	5287/4629
MW2-A	vs.	Control-A	Uterus	NDL	PR	0.57	65.1/60.4	5198/4629
MW1-B	vs.	Control-B	Uterus	NDL	PR	0.97	63.3/62.6	5571/4730
MW2-B	vs.	Control-B	Uterus	NDL	PR	0.87	63.4/62.6	5300/4730
Control-B*	vs.	Control-A	Uterus	NDL	PR	$p<0.05/p<0.05$	62.6/60.4	4730/4629
MW1-A	vs.	Control-A	Uterus	NDL	Ki67	$p<0.05$	1.2/1.8	84/109
MW2-A	vs.	Control-A	Uterus	NDL	Ki67	$p<0.05$	2.4/1.8	172/109
MW1-B	vs.	Control-B	Uterus	NDL	Ki67	0.94	3.3/2.5	221/163
MW2-B	vs.	Control-B	Uterus	NDL	Ki67	0.47	1.8/2.5	142/163
Control-B*	vs.	Control-A	Uterus	NDL	Ki67	0.42/0.42	2.5/1.8	163/109
MW1-A	vs.	Control-A	Uterus	SSM2	ER	0.52	58.1/59.7	6153/4572
MW2-A	vs.	Control-A	Uterus	SSM2	ER	0.83	51.0/59.7	4675/4572
MW1-B	vs.	Control-B	Uterus	SSM2	ER	0.42	72.1/69.0	7000/6097
MW2-B	vs.	Control-B	Uterus	SSM2	ER	0.05	61.6/69.0	5797/6097
Control-B*	vs.	Control-A	Uterus	SSM2	ER	0.87/ $p<0.05$	69.0/59.7	6097/4572
MW1-A	vs.	Control-A	Uterus	SSM2	PR	1.00	34.2/33.3	2899/1670
MW2-A	vs.	Control-A	Uterus	SSM2	PR	1.00	32.0/33.3	2474/1670
MW1-B	vs.	Control-B	Uterus	SSM2	PR	1.00	61.4/51.8	6595/3567
MW2-B	vs.	Control-B	Uterus	SSM2	PR	$p<0.05$	18.3/51.8	1647/3567
Control-B*	vs.	Control-A	Uterus	SSM2	PR	0.73/ $p<0.05$	51.8/33.3	3567/1670
MW1-A	vs.	Control-A	Uterus	SSM2	Ki67	0.47	4.5/6.9	402/451
MW2-A	vs.	Control-A	Uterus	SSM2	Ki67	0.68	9.5/6.9	723/451
MW1-B	vs.	Control-B	Uterus	SSM2	Ki67	0.99	7.6/6.1	635/427
MW2-B	vs.	Control-B	Uterus	SSM2	Ki67	0.42	5.8/6.1	453/427
Control-B*	vs.	Control-A	Uterus	SSM2	Ki67	0.73/ $p<0.05$	6.1/6.9	427/451

*Control to Control: 1st number "one-sided" KS-test; 2nd number "two-sided" KS-test.

**Total percent positive values from Table 1.

***Total cell density values from Table 2.

(Cardiff et al. 2013). The lack of sufficient tissue for the MW2-A sample made the results more difficult to interpret because the MW1-A (tumor A) and the MW2-B (tumor B) samples demonstrated $p<0.05$. The MW1-B sample had an excellent correlation to its control. The Control-B to -A correlation for the two-sample KS test was $p<0.05$, indicating a high degree of biological variation between the two tumors (Table 3). The Ki67 correlation of microwave-to-control results for all samples was good, but the two-sample KS test for the control-to-control comparison was $p<0.05$. This result indicated a high degree of biological variation between the tumors for this marker, which is consistent with the findings of a recent study (Cardiff et al. 2013).

The microwave results for all three uterine markers (ER, PR and Ki67) indicated good correlation with their respective controls except for MW2-B for ER ($p<0.05$) and PR ($p<0.05$). All the control-to-A comparisons for the two-sample KS tests resulted in $p<0.05$, but good correlation for the alternate hypothesis (Table 4).

Overview of KS test Results

Taken as a whole, these results demonstrate that (1) the KS test provides statistical evidence of biological variance between samples; (2) the KS test can detect small changes in antigenicity between samples fixed using different techniques; and (3) the MW protocols, with few

exceptions, did not reduce antigenicity in the tissues analyzed.

Microscopic Evaluation of IHC4

The four criteria set forth in the Materials & Methods for a microscopic examination—(1) stain localization, 2) stain uniformity, 3) background staining and 4) diagnostic/prognostic value—were met by both microwave and conventional/control fixation. The three nuclear antigens (ER, PR, and Ki67) presented three different intensity patterns for their respective labeling of the tumors from the NDL and SSM2 models (Table 1, Figs. 3–4, Supplemental Table 1, Supplemental Figs. 1–42). Tumor ER labeling in the SSM2 model for all samples was almost exclusively 1+ intensity, which was in contrast with the tumor SSM2 PR labeling, which presented a dominant 3+ intensity for all samples (see Tables 1–2, Fig. 4, Supplemental Figs. 25–36). The NDL tumors presented low percentage ER/PR labeling for all samples, which was evident in the percent positive labeling data (Table 1), line plots (Fig. 1), cell density data (Table 2) and Fig. 3. The Ki-67 tumor labeling for all samples in both models presented a speckled nuclear labeling pattern with relative uniformity of all labeling intensities (Tables 1–2, Figs. 3–4, Supplemental Table 1, Supplemental Figs. 13–18 and 37–42).

The ErbB2/Her2 staining in the NDL model presented similar intensities of label for all samples (Tables 1–2, Fig. 3, Supplemental Table 1, Supplemental Figs. 19–24). From the microscopic examination we concluded that MA methods of fixation tended to have less background. This finding was based on the blue counterstain (hematoxylin) contrast to the brown (DAB) IHC4 results, which overall appeared sharper in the MA fixations than the controls.

Summary of Results

These results combined empirical observation made by experts with multiple methods of quantitative comparison. The KS test results (Tables 3–4) provided the means to statistically compare the quantitative results embodied in the line plots. The line plots provided a graphical representation of the percent positive data, and the resulting cell density data used for the plots provided a more in depth examination of the percent positive data. The microscopic evaluation of the slides provided a trained eye to agree or disagree with the quantitative results.

Discussion

The results for this study were produced using image analysis (QIA of WSI), evaluated using statistics (KS test) and corroborated using the current gold standard—a microscopic examination by a trained pathologist. This entire process

was used to compare hormone receptor antigenicity between microwave-assisted formalin fixation and standard formalin fixation. The KS test results (Tables 3–4) provide the means to better understand the QIA components (Tables 1–2, Figs. 1–2) used in the study. The “two-sided” hypothesis of the KS test provided the mechanism to assess biological variance between tumors and within the uterine tissues from the NDL and SSM2 tumor models. No single approach could provide a definitive determination of retained antigenicity. As an example, the NDL Her2 nonconformance was evident in the light microscopic examination (results not shown), the line plots of Tumor A and B Controls (Fig. 1) and by the >30% difference in 2+ labeling intensity and the >20% difference in the 1+ intensity values (Table 1). However, the differences between MW1-A/MW2-A and the respective control fixations for uterine results were not apparent from any of the other results (Figs. 1–2, Tables 1–4), or even by light microscopic examination.

The QIA tools described here and in earlier works (Cardiff et al. 2013) serve to remove interobserver variability and thus provide a more reproducible approach for the quantification of labeling intensities. Although QIA may not yet be fully optimized or proven to give the best possible answer, it is well suited to measure the similarities in tissue antigenicity between samples. In the small sample sets used for this study, the binned histogram data provided the data sets necessary to do the statistical analysis and line plot visualization. The known heterogeneity of the tumors in the luminal SSM2 model (Cardiff et al. 2013) made direct comparisons more difficult for PR and Ki67 and this heterogeneity appeared to be present in the uterine PR and Ki67 *p* values from the “two-sided” KS test. The SSM2 PR uterine results were the least reliable data set, tumor or uterine, of this study based on the differences in percent positive and cell density values, but not based on the KS test “one-sided less than” alternative hypothesis.

The NDL breast cancer model proved to be the most reliable model to compare techniques based on QIA and KS test results. As an additional advantage, it was the only model that displayed prognostically relevant ErbB2/Her2 values (Cardiff et al. 2013).

The use of a less heterogeneous and well-characterized model system (NDL) in conjunction with QIA of WSI has many advantages. It tests each aspect of a laboratory’s SOP, from tissue acquisition to final post-staining of the immunelabeled slide. Model systems, such as the NDL/SSM2 mouse models of breast cancer, which have been adapted for QIA of WSI (Cardiff et al. 2013), are valuable tools in the evaluation of new methods or changes to existing methods. A significant advantage of QIA of WSI is that a small sample size yields a large number of data points. When the points are integrated together to form the line plots, the raw data can then be used for the KS test or the similar Anderson–Darling test (Stephens 1974).

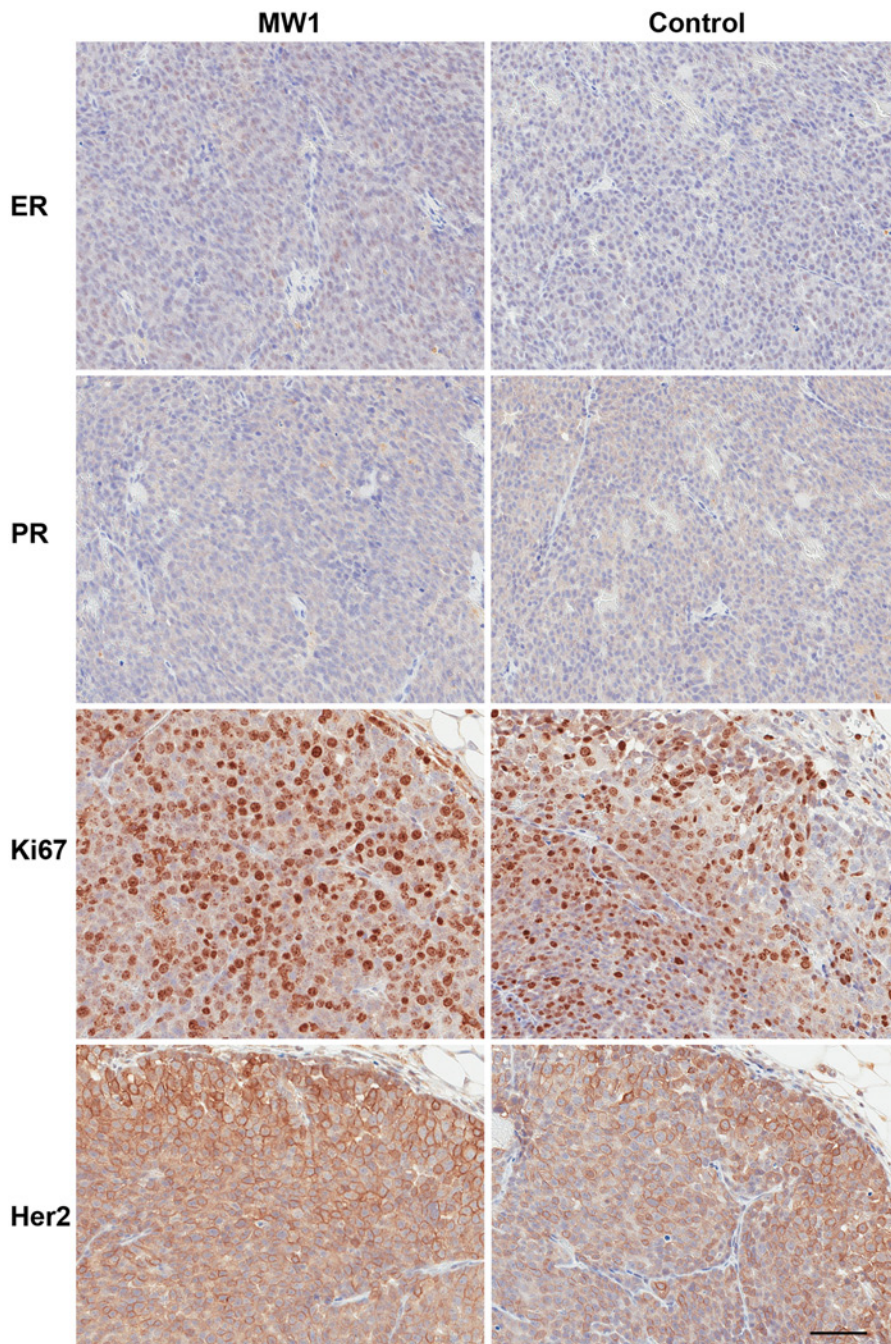


Figure 3. Representative photomicrographs of the tumor four-antigen panel (IHC4) immunohistochemistry from the NDL tumors. The images for microwave protocol #1 (MW1, see Materials & Methods) are MW1-A (tumor A) for estrogen receptor (ER) and progesterone receptor (PR) with their respective controls. The Ki67 and human epidermal growth factor receptor 2 (Her2) images are MW1-B (tumor B) with their respective controls. The photomicrographs are characteristic of the overall IHC4 staining patterns, intensities and background observed microscopically with this model. Scale bar, 50 μ m.

Although we believe that this report, along with previously published data (Galvez et al. 2006; Gagna et al. 2007), demonstrates the feasibility and usefulness of the microwave for fixing tissue samples, we are aware that, especially in the clinical setting, adopting new technology requires re-validation of antibodies and techniques (Hammond et al. 2010). We are also aware that, although avoiding decreased antigenicity is obviously beneficial, increased antigenicity can also be problematic, especially for tests such as Dako's Herceptest™, where increases in

antigenicity can lead to false positives. The overall results of this study indicate that the most reliable microwave protocol was the single wattage (150W: MW1-A and MW1-B) technique; the KS test validates this conclusion based on MW2 $p < 0.05$ results.

The microscopic examination of the MA fixation indicated that, in many cases, the MA-fixed tissue had empirically better staining quality. It is possible that for a less than optimal fixation using other fixatives, the use of MA fixation might “rescue” the fixation quality and improve

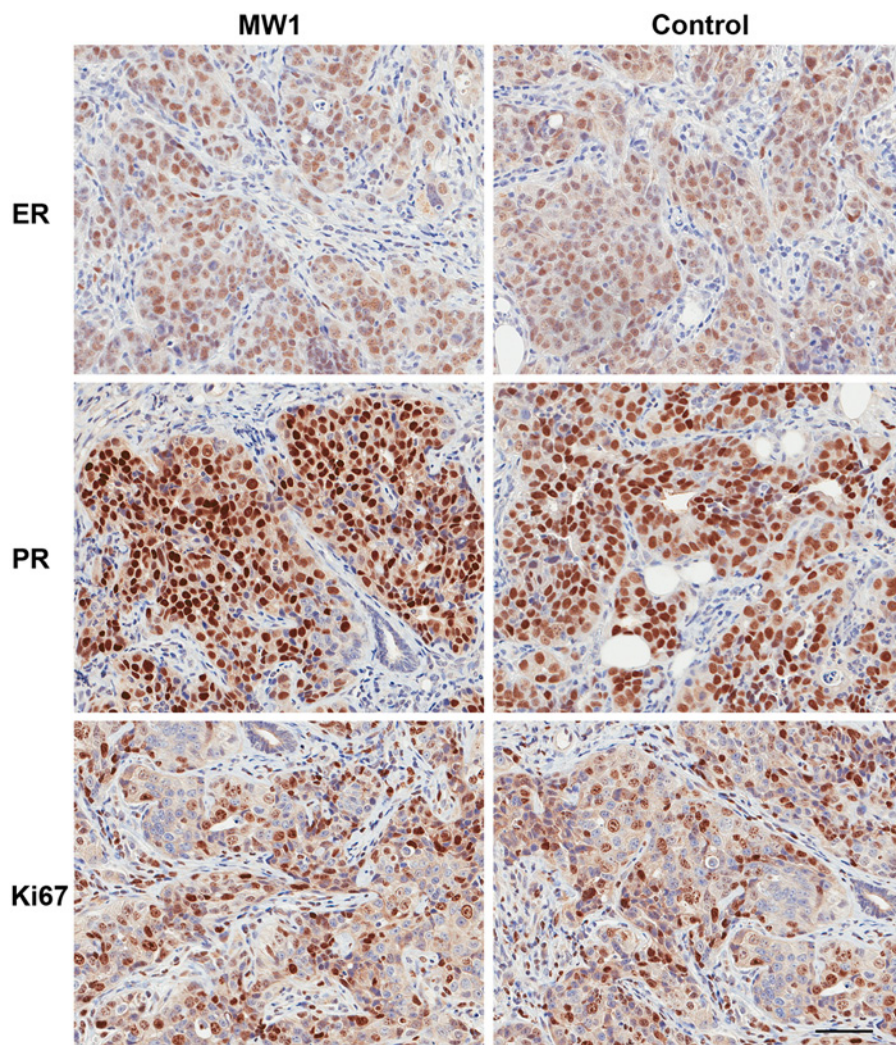


Figure 4. Representative photomicrographs of the tumor four-antigen panel (IHC4) immunohistochemistry from the SSM2 tumors. The images for microwave protocol #1 (MW1; see Materials & Methods) are MW1-A (tumor A) for estrogen receptor (ER) and MW1-B (tumor B) for progesterone receptor (PR) and Ki67 with their respective controls. The SSM2 model is Her2 negative. The photomicrographs are characteristic of the overall IHC4 staining patterns, intensities and background observed microscopically with this model. Scale bar, 50 μ m.

antigenicity. However, previous results (Galvez et al. 2006), suggest that epitope retrieval is still required when using MA fixation, so that step cannot be avoided.

In previous research, we demonstrated that an MA NBF fixation was a combination of controlled wattage and fixative temperature (Galvez et al. 2006; Gagna et al. 2007) and that electron microscopy confirmed that MA methods can reduce fixation times (Galvez et al. 2006). NBF penetrates tissues at a rate of roughly 1 mm per hour, but the fixation process is a chemical reaction that requires 24 hours to complete at room temperature (Fox et al. 1985; Goldstein et al. 2003; Yaziji et al. 2008). An elevation in temperature is clearly not the mechanism behind a reduction in MA NBF fixation times in this research (Fox et al. 1985). At this time, we can only speculate that the presence of 2.45 GHz microwave energy causes a reduction in the activation energy required for NBF crosslinking to normally take place, independent of heat.

Our results indicate that a single wattage approach is best for the IHC4 of breast cancer. Microwave fixation is

far quicker than conventional methods and the results from QIA of WSI clearly indicate equal or better retention of antigenicity for the IHC4. Controlled microwave NBF fixation is a promising technology for the standardization of NBF fixation times.

Acknowledgments

The authors wish to acknowledge Dr. Anthony Nasr for his ongoing support over the years. The SSM2 and NDL mouse tissues were a gift from Dr. A.D. Borowsky. We thank Judith E. Walls for technical histological work, Ted Pella, Inc. for their support in this research, and Ben Schwartz for technical support. Lawrence Young passed away during the preparation of the manuscript, but made significant contributions to the study design, execution, and analysis.

Declaration of Conflicting Interests

The author(s) declared the following potential conflicts of interest with respect to the research, authorship, and/or publication of this article: Richard T. Giberson is the manager of biomedical R&D

for Ted Pella Inc. (Redding, CA), the manufacturer of the microwave used in this study. Mr. Giberson is a recognized expert in the field of microwave biomedical research, has authored numerous papers, and presented numerous workshops on microwave processing techniques. Ted Pella, Inc. provided the cost of slide preparation and whole slide imaging for this study. All other authors, (JAE, LJTY, NEH, RDC) have no conflicts of interest or competing financial interests.

Funding

The author(s) disclosed receipt of the following financial support for the research, authorship, and/or publication of this article: The research described here was supported in part by Athena Breast Health Network through the Safeway Foundation and University of California Office of the President [Grants U01-CA141582, U01-CA141541] and from the National Cancer Institute's Mouse Models of Human Cancers Consortium [U01 CA105490-01] (RDC, JAE, NEH).

References

- Allred DC, Harvey JM, Berardo M, Clark GM (1998). Prognostic and predictive factors in breast cancer by immunohistochemical analysis. *Mod Pathol* 11:155-168.
- Cardiff RD, Hubbard NE, Engelberg JA, Munn RJ, Miller CH, Walls JE, Chen JQ, Velásquez-García HA, Galvez JJ, Bell KJ, Beckett LA, Li YJ, Borowsky AD (2013). Quantitation of fixative-induced morphologic and antigenic variation in mouse and human breast cancers. *Lab Invest* 93:480-497.
- Chan SR, Vermi W, Luo J, Lucini L, Rickert C, Fowler AM, Lonardi S, Arthur C, Young LJ, Levy DE, Welch MJ, Cardiff RD, Schreiber RD (2012). STAT1-deficient mice spontaneously develop estrogen receptor α -positive luminal mammary carcinomas. *Breast Cancer Res* 14:R16.
- Cuzick J, Dowsett M, Pineda S, Wale C, Salter J, Quinn E, Zabaglo L, Mallon E, Green AR, Ellis IO, Howell A, Buzdar AU, Forbes JF (2011). Prognostic value of a combined estrogen receptor, progesterone receptor, Ki-67, and human epidermal growth factor receptor 2 immunohistochemical score and comparison with the Genomic Health recurrence score in early breast cancer. *J Clin Oncol* 29:4273-4278.
- Fox CH, Johnson FB, Whiting J, Roller PP (1985). Formaldehyde Fixation. *J Histochem Cytochem* 33:845-853.
- Gagna CE, Kuo H-R, Chan NJ, Mitacek EJ, Spivak A, Pasquariello TD, Balgobin C, Mukhi R, Lambert WC (2007). Novel DNA staining method and processing technique for the quantification of undamaged double-stranded DNA in epidermal tissue sections by PicoGreen probe staining and microspectrophotometry. *J Histochem Cytochem* 55:999-1014.
- Galvez JJ, Giberson RT, Cardiff RD (2006). The role of microwave radiation in reducing formaldehyde fixation times demonstrated in liver. *J Histotechnol* 29:113-121.
- Giberson R, Elliott D (2001). Microwave-Assisted Formalin Fixation of Fresh Tissue: A Comparative Study. In: RT Giberson & RSJ Demaree, editors. *Microwave Techniques and Protocols*. Totowa, NJ: Humana Press p. 191-208.
- Goldstein NS, Ferkowicz M, Odish E, Mani A, Hastah F (2003). Minimum formalin fixation time for consistent estrogen receptor immunohistochemical staining of invasive breast carcinoma. *Am J Clin Pathol* 120:86-92.
- Gown AM (2008). Current issues in ER and HER2 testing by IHC in breast cancer. *Mod Pathol* 21:S8-S15.
- Hammond MEH, Hayes DF, Dowsett M, Allred DC, Hagerty KL, Badve S, Fitzgibbons PL, Francis G, Goldstein NS, Hayes M, Hicks DG, Lester S, Love R, Mangu PB, McShane L, Miller K, Osborne CK, Paik S, Perlmutter J, Rhodes A, Sasano H, Schwartz JN, Sweep FC, Taube S, Torlakovic EE, Valenstein P, Viale G, Visscher D, Wheeler T, Williams RB, Wittliff JL, Wolff AC (2010). American Society of Clinical Oncology/College of American Pathologists guideline recommendations for immunohistochemical testing of estrogen and progesterone receptors in breast cancer. *J Clin Oncol* 28:2784-2795.
- Kolmogorov A (1933). Sulla determinazione empirica di una legge di distribuzione. *G Ist Ital Attuari* 4:83.
- Kurosumi M (2007). Immunohistochemical assessment of hormone receptor status using a new scoring system (J-Score) in breast cancer. *Breast Cancer* 14:189-193.
- Leake R, Barnes D, Pinder S, Ellis I, Anderson L, Anderson T, Adamson R, Rhodes T, Miller K, Walker R (2000). Immunohistochemical detection of steroid receptors in breast cancer: a working protocol. UK Receptor Group, UK NEQAS, The Scottish Breast Cancer Pathology Group, and The Receptor and Biomarker Study Group of the EORTC. *J Clin Pathol* 53:634-635.
- McClelland RA, Finlay P, Walker KJ, Nicholson D, Robertson JF, Blamey RW, Nicholson RI (1990). Automated quantitation of immunocytochemically localized estrogen receptors in human breast cancer. *Cancer Res* 50:3545-3550.
- Nofech-Mozes S, Vella ET, Dhesy-Thind S, Hagerty KL, Mangu PB, Temin S, Hanna WM (2012). Systematic review on hormone receptor testing in breast cancer. *Appl Immunohistochem Mol Morphol* 20:214-263.
- PM, Siegel ED, Ryan RD, Cardiff & WJ, Muller (1999). Elevated expression of activated forms of Neu/ErbB-2 and ErbB-3 are involved in the induction of mammary tumors in transgenic mice: implications for human breast cancer. *EMBO J* 18:2149-2164.
- Stephens MA (1974). EDF statistics for goodness of fit and some comparisons. *J Am Stat Assoc* 69: 730-737.
- Tong LC, Nelson N, Tsurugiannis J, Mulligan AM (2011). The effect of prolonged fixation on the immunohistochemical evaluation of estrogen receptor, progesterone receptor, and HER2 expression in invasive breast cancer: a prospective study. *Am J Surg Pathol* 35:545-552.
- von Wasielewski R, Mengel M, Nolte M, Werner M (1998). Influence of Fixation, Antibody Clones, and Signal Amplification on Steroid Receptor Analysis. *Breast J* 4:33-40.
- Wolff AC, Hammond MEH, Schwartz JN, Hagerty KL, Allred DC, Cote RJ, Dowsett M, Fitzgibbons PL, Hanna WM, Langer A, McShane LM, Paik S, Pegram MD, Perez EA, Press MF, Rhodes A, Sturgeon C, Taube SE, Tubbs R, Vance GH, van de Vijver M, Wheeler TM, Hayes DF; American Society of Clinical Oncology; College of American Pathologists (2007). American Society of Clinical Oncology/College of American Pathologists guideline recommendations for human epidermal growth factor receptor 2 testing in breast cancer. *J Clin Oncol* 25:118-145.

Yaziji H, Taylor CR, Goldstein NS, Dabbs DJ, Hammond EH, Hewlett B, Floyd AD, Barry TS, Martin AW, Badve S, Baehner F, Cartun RW, Eisen RN, Swanson PE, Hewitt SM, Vyberg M, Hicks DG; Members of the Standardization

Ad-Hoc Consensus Committee (2008). Consensus recommendations on estrogen receptor testing in breast cancer by immunohistochemistry. *Appl Immunohistochem Mol Morphol* 16:513-520.